Structural basis for negative cooperativity within agonist-bound TR:RXR heterodimers

Balananda-Dhurjati K. Putcha[a,1], Edward Wright[a,1], Joseph S. Brunzelle[b], and Elias J. Fernandez[a,2]

[a]Biochemistry, Cellular and Molecular Biology, University of Tennessee, Knoxville, TN 37996; and [b]Department of Molecular Pharmacology and Biological Chemistry, Life Sciences Collaborative Access Team, Northwestern University Feinberg School of Medicine, Chicago, IL 60611

Edited by Ronald M. Evans, The Salk Institute for Biological Studies, La Jolla, CA, and approved March 6, 2012 (received for review December 1, 2011)

Thyroid hormones such as 3,3′,5 triiodo-L-thyronine (T3) control numerous aspects of mammalian development and metabolism. The actions of such hormones are mediated by specific thyroid hormone receptors (TRs). TR belongs to the nuclear receptor family of modular transcription factors that binds to specific DNA-response elements within target promoters. These receptors can function as homo- or heterodimers such as TR:9-*cis* retinoic acid receptor (RXR). Here, we present the atomic resolution structure of the TRα•T3:RXRα•9-*cis* retinoic acid (9c) ligand binding domain heterodimer complex at 2.95 Å along with T3 hormone binding and dissociation and coactivator binding studies. Our data provide a structural basis for allosteric communication between T3 and 9c and negative cooperativity between their binding pockets. In this structure, both TR and RXR are in the active state conformation for optimal binding to coactivator proteins. However, the structure of TR•T3 within TR•T3:RXR•9c is in a relative state of disorder, and the observed kinetics of binding show that T3 dissociates more rapidly from TR•T3:RXR•9c than from TR•T3:RXR. Also, coactivator binding studies with a steroid receptor coactivator-1 (receptor interaction domains 1–3) fragment show lower affinities (K_a) for TR•T3:RXR•9c than TR•T3:RXR. Our study corroborates previously reported observations from cell-based and binding studies and offers a structural mechanism for the repression of TR•T3:RXR transactivation by RXR agonists. Furthermore, the recent discoveries of multiple endogenous RXR agonists that mediate physiological tasks such as lipid biosynthesis underscore the pharmacological importance of negative cooperativity in ligand binding within TR:RXR heterodimers.

allostery | thyroid receptor

In the simplest model for transactivation, agonist binding to either receptor in the nuclear receptor (NR) heterodimer must activate downstream genes. However, when treated with both agonists at one time, NR:9-*cis* retinoic acid receptor (RXR) complexes exhibit diverse transcriptional responses (1, 2) and provide additional layers of regulation of the transcriptional activity of heterodimeric NRs. For instance, agonists for either liver X receptor (LXR) or RXR can transactivate the LXR:RXR heterodimer and double transcriptional levels when these agonists are used in concert (2). However, full activity of the thyroid hormone receptor (TR):RXR heterodimer is only in response to 3,3′,5 triiodo-L-thyronine (T3) alone and cannot be independently achieved by the RXR agonist. Furthermore, transactivation levels of TR•T3:RXR are lower than optimal in the presence of the RXR agonist (1, 3). This negative cooperativity in TR:RXR heterodimers is in sharp contrast to the positive control exerted by the RXR agonist on retinoic acid receptor (RAR):RXR transactivation (4). NRs such as TR and RXR are modular proteins with recognizable domains that perform distinct functions in multiple oligomeric states (5, 6). Although the DNA binding domain (DBD) recognizes specific DNA promoter elements (5), agonist ligand recognition and accompanying conformational changes occur largely within the ligand binding domain (LBD) (7). The inactive state conformations of NR have been described by the structures of unliganded RXR (8), in antagonist-bound peroxisome proliferator-activated receptor γ (PPARγ) (9), or inverse agonist-bound constitutive androstane receptor (CAR) (10) LBDs, whereas the RXR•9c LBD structure (11) is the canonical representation of the NR active state conformation.

Results and Discussion

9c Allosterically Disrupts TR Structure. Although TR:RXR plays a vital role in developmental and metabolic processes (12, 13), the molecular mechanisms of transactivation are unknown. In this study, we have examined the structural basis of negative cooperativity between the agonists for TR:RXR from a crystal structure of the TR•T3:RXR•9c LBD determined at 2.95 Å. Phasing for structure determination was obtained using a combination of molecular replacement and anomalous scattering from iodine in the T3 ligand (Table S1). There is a single TR•T3:RXR•9c LBD within the crystallographic asymmetric unit (Fig. 1*A*). The overall structures of TR and RXR within TR•T3:RXR•9c are similar to previously determined TRα•T3 (14) (rmsd = 0.65 Å) and RXRα•9c (11) (rmsd = 0.56 Å), suggesting that there are minimal changes to the conformation of the receptor on heterodimerization. However, there are two unique and interrelated features in the TR•T3:RXR•9c structure that form the basis of the 9c-initiated allosteric effects on the activity of this complex. First, the electron density ($2|F_o| - |F_c|$ contoured at 1× SD) of the TR subunit of TR•T3:RXR•9c is frequently discontinuous, and second, the density of RXR within the same complex is mostly uninterrupted (Fig. S1). Regions with the most significant disorder in electron density are within the T3 ligand binding pocket and the coactivator binding site of TR (Fig. 1*B*). Also, the absence of density is largely from the side chains of residues, whereas the main chain density is strong and continuous. We sought to validate the presence of these side chains by first substituting the problematic residues with alanine and then calculating $|F_o| - |F_c|$ coefficient electron density maps. The presence of strong (3× SD) peaks in the $|F_o| - |F_c|$ coefficient electron density maps (Fig. 1*C*) confirms that the observed disordered density is not a crystallographic artifact and is analogous to previous reports of local or global dynamics within proteins (15) and protein•ligand (16) structures that manifest as either high individual atomic temperature factors (B factors) or discontinuous electron density (17). Finally, by occupancy refinement of only T3 (occupancy = 0.70) and 9c (occupancy = 0.99), we were able to remove the negative electron density on

Author contributions: E.J.F. designed research; B.-D.K.P., E.W., and E.J.F. performed research; E.J.F. contributed new reagents/analytic tools; B.-D.K.P., E.W., J.S.B., and E.J.F. analyzed data; and B.-D.K.P. and E.J.F. wrote the paper.

The authors declare no conflict of interest.

This article is a PNAS Direct Submission.

Data deposition: The crystallography, atomic coordinates, and structure factors have been deposited in the Protein Data Bank, www.pdb.org (PDB ID code 3UVV).

[1]B.-D.K.P. and E.W. contributed equally to this work.

[2]To whom correspondence should be addressed. E-mail: Elias.Fernandez@utk.edu.

This article contains supporting information online at www.pnas.org/lookup/suppl/doi:10.1073/pnas.1119852109/-/DCSupplemental.

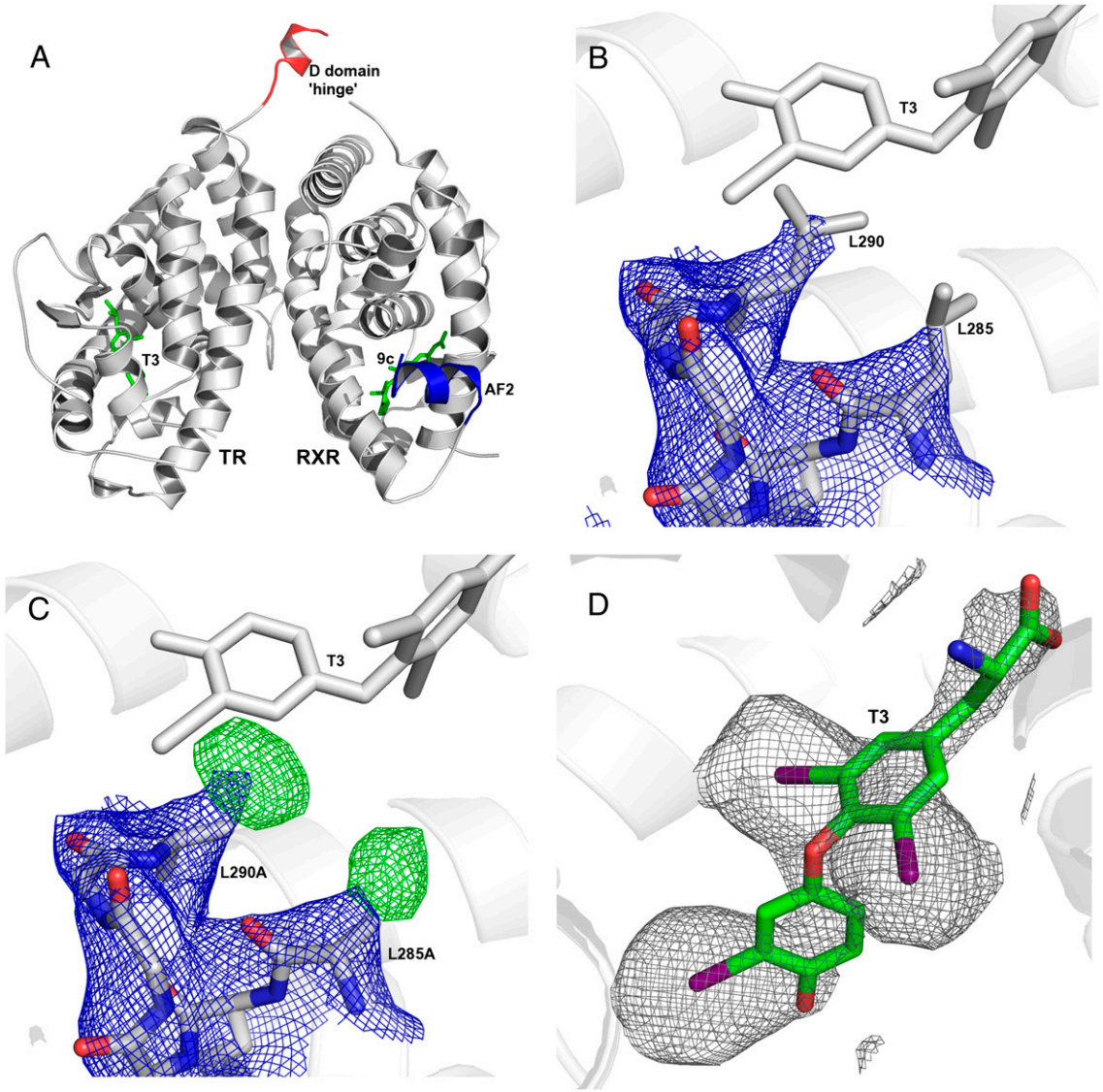

Fig. 1. Structural basis for allostery in TR•T3:RXR•9c. (*A*) C_α trace (white) of the conformation of the TR•T3:RXR•9c LBD complex. The TR subunit encompasses residues 148–408 and includes the hinge (D domain; shown in red). The RXR subunit includes residues 225–462, and the C-terminal helix H12 (AF2) is shown in blue. T3 and 9c are shown in green. (*B*) $2|F_o| - |F_c|$ coefficient electron density contoured at 1.0× σ of residues 285–290 within the TR ligand binding pocket shows that the side chain density is missing for several amino acids. (*C*) $2|F_o| - |F_c|$ (blue, 1× σ) and $|F_o| - |F_c|$ (green, 3× σ) coefficient electron density of (L285A, L290A)TR•T3:RXR•9c. The $|F_o| - |F_c|$ density confirms the presence of the missing *Leu* side chains. (*D*) T3 superimposed on $2|F_o| - |F_c|$ coefficient electron density contoured at 1.5× σ. Only the occupancies of both T3 and 9c were refined independently of the thermal parameters (B factors) of TR•T3:RXR•9c.

T3 ($2|F_o| - |F_c|$ density is shown in Fig. 1*D*). Thus, it is very likely that the disorder in TR•T3:RXR•9c derives from an increase in the local dynamics and loosening of the TR•T3 moiety.

T3 Dissociation Rates Increase in TR•T3:RXR•9c. A consequence of ligand-induced loosening of protein structures is a change in ligand binding parameters (18). Also, recent analyses of homodimeric progesterone receptor•ligand complexes show that interligand cross-talk can regulate transactivation (19). Therefore, to study the role of 9c within TR•T3:RXR•9c and determine if the observed disorder can influence T3 binding, we measured both the equilibrium binding of T3 to TR:RXR•9c and dissociation kinetics of this agonist from the TR•T3:RXR•9c complex. Indeed, the measured dissociation rate of ^{125}I-labeled T3 from TR•T3:RXR•9c ($t_{1/2}$ = 8.2 min) is greater than two times the rate of T3 dissociation from TR•T3:RXR ($t_{1/2}$ = 20.7 min) (Fig. 2*A*). This result shows that, although the T3 dissociation rate is unaffected by heterodimerization with RXR (20), the presence of 9c can increase the rate at which T3 dissociates from TR•T3:RXR•9c. Furthermore, the equilibrium binding affinity of T3 for TR:RXR (K_d = 0.35 nM) is greater than TR:RXR•9c (K_d = 0.61 nM) (Fig. 2*A*, *Inset*), suggesting a stronger TR•T3 complex in the absence of 9c within TR:RXR than in TR•T3:RXR•9c. Collectively, these results indicate that TR within TR•T3:RXR•9c (this structure) is relatively destabilized compared with TR•T3:RXR, and this conclusion is not evident from the overall rmsd from published TR structures (14).

Steroid Receptor Coactivator-1 Shows Diminished Affinity to TR•T3:RXR•9c LBDs. It is well-established that T3 agonist binding in TR is accompanied by conformational changes that are mostly within the C-terminal helix H12 (AF2 domain) (14). In TR•T3:RXR•9c, the AF2 domain is in the typical NR active state conformation (21) (Fig. 1*A*) for binding to coactivator proteins

BIOCHEMISTRY

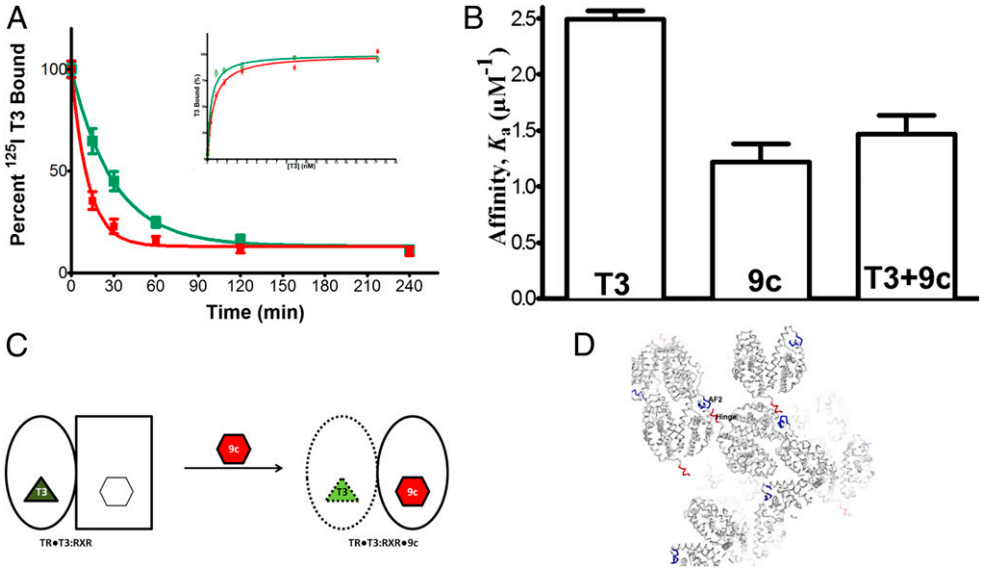

Fig. 2. Biochemical basis for negative cooperativity in TR•T3:RXR•9c. (*A*) Competitive dissociation of bound ^{125}I-T3 from TR•T3:RXR (green trace, $t_{1/2}$ = 20.7 ± 3.4 min) and TR•T3:RXR•9c (red trace, $t_{1/2}$ = 8.2 ± 3.8 min) LBD. (*Inset*) Equilibrium binding of ^{125}I-T3 to TR:RXR (green trace, K_d = 0.35 ± 0.071 nM) and TR:RXR•9c (red trace, K_d = 0.61 ± 0.11 nM). (*B*) Binding of SRC1(RID1–3), residues 617–769, to TR•T3:RXR, TR:RXR•9c, and TR•T3:RXR•9c determined by ITC. (*C*) Summary of the allosteric process shows that 9c binding to TR•T3:RXR induces conformational changes in both RXR [unliganded (rectangle) to 9c-bound (oval) and from a more rigid TR•T3 (oval) to a more dynamic state TR•T3 (dashed oval)]. (*D*) Crystal packing of TR•T3:RXR•9c in the C222$_1$ unit cell. The only crystal packing interactions are between the N-terminal extension of TR LBD (red) and the C-terminal helix H12 of RXR (blue) of the neighboring TR•T3:RXR•9c in an adjacent asymmetric unit.

such as the steroid receptor coactivator-1 (SRC1) (22). However, as observed with the ligand binding pocket, the electron density of side chains of AF2 within the TR coactivator binding site is also disordered. Earlier studies have shown that the optimal recruitment of coactivators by NRs requires the most favorable conformation of AF2, and small changes in the dynamics of this domain can have profound effects on both coactivator binding affinities and transactivation levels (23). Other findings have established a direct relationship between the potency of the TR agonist and the binding affinity of coactivator in TRβ (20). For that reason, we examined the effectiveness of TR•T3:RXR•9c in binding coactivator by isothermal titration calorimetry (ITC). In this test, we compared the affinity of TR•T3:RXR•9c and TR•T3:RXR with an SRC1 fragment (residues 617–769) that encompasses the receptor interaction domain [RID; SRC1 (RID1–3)] of this coactivator. The data that we obtained showed that the affinity of SRC1(RID1–3) is lower in TR•T3:RXR•9c (K_d = 0.68 ± 0.7 μM) than in TR•T3:RXR (K_d = 0.4 ± 0.04 μM) (Fig. 2*B* and Fig. S2). Similar affinity measurements between a TR DBD-hinge-LBD domain construct and SRC1 have shown a similar binding pattern (3). Thus, when taken together, our data indicate that the allostery initiated by 9c leads to the destabilization of TR within the TR•T3:RXR•9c complex, thereby diminishing T3 binding affinity and coactivator recruitment and repressing transactivation.

Crystal Packing Interactions Suggest That the TR D Domain Can Mimic the SRC1 LXXLL Motif. Overall, the structure of the TR•T3:RXR•9c heterodimer most closely resembles the RAR:RXR LBD (24) (Fig. S1*A*). Both TR and RAR have the same angular orientation to RXR (Fig. S3*A*), with comparably small and homologous heterodimer interfaces (TR:RXR = 971 Å^2 and RAR:RXR = 959 Å^2) (Fig. S3*B* and Table S2). The solvent content within the TR•T3:RXR•9c crystal is ∼70% (Table S1), and thus, the majority of the molecular surface is exposed to solvent channels. Consequently, electron density for the loop that links helix H1 to helix H2 in both the TR and RXR subunits is poor, and this region has also been shown to be relatively mobile in other NR structures (11, 25). The only observable crystal-packing interactions occur between the N-terminal extension of the TR LBD from one TR•T3:RXR•9c and the RXR AF2 of TR•T3:RXR•9c in the neighboring asymmetric unit, forming an indefinitely extended pattern of interacting TR•T3:RXR•9c heterodimers (Fig. 2*D* and Fig. S4*A*). This N-terminal extension encompasses the linker (D domain) between the TR DBD and LBD, has an amino acid sequence that is homologous to the SRC1 RID (Fig. S4*B*), and adopts an interacting helical conformation similar to the SRC1-derived LXXLL peptide commonly used in cocrystallization with nuclear receptors (25) (Fig. S4*C*). A similar self-association within crystallized TRα has been previously observed (26), prompting us to test if this TR ↔ RXR interaction contributes to the allostery within TR•T3:RXR•9c. We generated a TR mutant, (M148K, I149K)TR, designed to disrupt the interheterodimeric TR ↔ RXR interaction and compared the transactivation profile of this mutant with the native TR:RXR complex. Because the pattern of transactivation of mutant and native protein is identical (Fig. S4*D*), we could not relate the crystal-packing interheterodimer interactions with the allostery of TR•T3:RXR•9c.

Conclusions

The data produced in our study propose that 9c functions as an allosteric repressor of TR:RXR transactivation by stimulating conformational changes within the complex. The familiar therapeutic use of T3 analogs (27) to compensate for disease state levels of T3 (and potentially, RXR agonists) as a consequence of mutations within the hormone transporters (28) and other regulatory pathways underscores the clinical importance of allostery in regulating TR transactivation. Also, the presence of RXR agonists emphasizes the delicate balance in the modulation of ligand-mediated transactivation of TR:RXR heterodimers (29, 30). The structural changes reported here are simply a global loosening of TR within TR•T3:RXR•9c, which results in a conformation that is indistinguishable from the free TR•T3 structure (14) using rmsd measurements. This loosening of TR is the

basis for a continuum of TR:RXR conformations that can result in a broad range of activity states. Additional efforts will illustrate the broader significance and underlying mechanism of cooperativity in other heterodimeric NR complexes.

Materials and Methods

Details are in *SI Materials and Methods*. We used BL21 DE3 *Escherichia coli* to overexpress the TR and RXR LBDs. After purification by affinity to an Ni-nitrilotriacetic acid (Ni-NTA) matrix, anion exchange, and size exclusion chromatography, the protein was concentrated and crystallized.

Protein from the BL21 DE3 cells was used for T3 binding and SRC1 coactivator recruitment assays. ^{125}I-T3 binding and dissociation assays were performed with and without 9c, and the data represent an average of measurements in triplicate. SRC1 binding was performed by ITC, with each titration containing 10–25 μM of the complex.

Transactivation studies were performed in CV-1 cells, and luciferase gene expression levels are used as a measure of TR:RXR activity.

ACKNOWLEDGMENTS. We thank Mr. William Alexander for mutagenesis of the TR D domain. We also thank Drs. Chris Dealwis, Barry Marc Forman, Robert Fletterick, Martin Privalsky, and Cherian Zachariah for critical reading of the manuscript and Dr. Herbert Samuels for discussions. We thank Ms. Nina Martyris for editing the manuscript. Funds were from National Institutes of Health–National Institute of Diabetes and Digestive and Kidney Diseases Grant DK066394 (to E.J.F.).

1. Forman BM, Umesono K, Chen J, Evans RM (1995) Unique response pathways are established by allosteric interactions among nuclear hormone receptors. *Cell* 81: 541–550.
2. Shulman AI, Larson C, Mangelsdorf DJ, Ranganathan R (2004) Structural determinants of allosteric ligand activation in RXR heterodimers. *Cell* 116:417–429.
3. Putcha BD, Fernandez EJ (2009) Direct interdomain interactions can mediate allosterism in the thyroid receptor. *J Biol Chem* 284:22517–22524.
4. Schulman IG, Li C, Schwabe JW, Evans RM (1997) The phantom ligand effect: Allosteric control of transcription by the retinoid X receptor. *Genes Dev* 11:299–308.
5. Mangelsdorf DJ, Evans RM (1995) The RXR heterodimers and orphan receptors. *Cell* 83:841–850.
6. Mengeling BJ, Lee S, Privalsky ML (2008) Coactivator recruitment is enhanced by thyroid hormone receptor trimers. *Mol Cell Endocrinol* 280:47–62.
7. Westin S, et al. (1998) Interactions controlling the assembly of nuclear-receptor heterodimers and co-activators. *Nature* 395:199–202.
8. Bourguet W, Ruff M, Chambon P, Gronemeyer H, Moras D (1995) Crystal structure of the ligand-binding domain of the human nuclear receptor RXR-alpha. *Nature* 375: 377–382.
9. Xu HE, et al. (2002) Structural basis for antagonist-mediated recruitment of nuclear co-repressors by PPARalpha. *Nature* 415:813–817.
10. Shan L, et al. (2004) Structure of the murine constitutive androstane receptor complexed to androstenol: A molecular basis for inverse agonism. *Mol Cell* 16:907–917.
11. Egea PF, et al. (2000) Crystal structure of the human RXRalpha ligand-binding domain bound to its natural ligand: 9-cis retinoic acid. *EMBO J* 19:2592–2601.
12. Ribeiro RC, et al. (1995) The molecular biology of thyroid hormone action. *Ann N Y Acad Sci* 758:366–389.
13. Yen PM (2001) Physiological and molecular basis of thyroid hormone action. *Physiol Rev* 81:1097–1142.
14. Wagner RL, et al. (1995) A structural role for hormone in the thyroid hormone receptor. *Nature* 378:690–697.
15. Artymiuk PJ, et al. (1979) Crystallographic studies of the dynamic properties of lysozyme. *Nature* 280:563–568.
16. Huber R (1987) Flexibility and rigidity, requirements for the function of proteins and protein pigment complexes. Eleventh Keilin memorial lecture. *Biochem Soc Trans* 15: 1009–1020.
17. Carroll MJ, et al. (2011) Direct detection of structurally resolved dynamics in a multiconformation receptor-ligand complex. *J Am Chem Soc* 133:6422–6428.
18. Williams DH, O'Brien DP, Sandercock AM, Stephens E (2004) Order changes within receptor systems upon ligand binding: Receptor tightening/oligomerisation and the interpretation of binding parameters. *J Mol Biol* 340:373–383.
19. Lusher SJ, et al. (2011) Structural basis for agonism and antagonism for a set of chemically related progesterone receptor modulators. *J Biol Chem* 286:35079–35086.
20. Jeyakumar M, Webb P, Baxter JD, Scanlan TS, Katzenellenbogen JA (2008) Quantification of ligand-regulated nuclear receptor corepressor and coactivator binding, key interactions determining ligand potency and efficacy for the thyroid hormone receptor. *Biochemistry* 47:7465–7476.
21. Huber BR, et al. (2003) Two resistance to thyroid hormone mutants with impaired hormone binding. *Mol Endocrinol* 17:643–652.
22. Moore JM, Guy RK (2005) Coregulator interactions with the thyroid hormone receptor. *Mol Cell Proteomics* 4:475–482.
23. Wright E, et al. (2011) Helix 11 dynamics is critical for constitutive androstane receptor activity. *Structure* 19:37–44.
24. Bourguet W, et al. (2000) Crystal structure of a heterodimeric complex of RAR and RXR ligand-binding domains. *Mol Cell* 5:289–298.
25. Suino K, et al. (2004) The nuclear xenobiotic receptor CAR: Structural determinants of constitutive activation and heterodimerization. *Mol Cell* 16:893–905.
26. Nascimento AS, et al. (2006) Structural rearrangements in the thyroid hormone receptor hinge domain and their putative role in the receptor function. *J Mol Biol* 360: 586–598.
27. Arsanjani R, McCarren M, Bahl JJ, Goldman S (2011) Translational potential of thyroid hormone and its analogs. *J Mol Cell Cardiol* 51:506–511.
28. Refetoff S, Dumitrescu AM (2007) Syndromes of reduced sensitivity to thyroid hormone: Genetic defects in hormone receptors, cell transporters and deiodination. *Best Pract Res Clin Endocrinol Metab* 21:277–305.
29. de Urquiza AM, et al. (2000) Docosahexaenoic acid, a ligand for the retinoid X receptor in mouse brain. *Science* 290:2140–2144.
30. Volakakis N, Joodmardi E, Perlmann T (2009) NR4A orphan nuclear receptors influence retinoic acid and docosahexaenoic acid signaling via up-regulation of fatty acid binding protein 5. *Biochem Biophys Res Commun* 390:1186–1191.